Biosensors and Bioelectronics 72 (2015) 326–331

Contents lists available at ScienceDirect

Biosensors and Bioelectronics

journal homepage: www.elsevier.com/locate/bios

A label-free fluorescent biosensor for ultratrace detection of terbium (III) based on structural conversion of G-quadruplex DNA mediated by ThT and terbium (III)

Qiang Chen [a,d], Junfeng Zuo [a], Jinfeng Chen [a], Ping Tong [a], Xiujuan Mo [d], Lan Zhang [a,*], Jianrong Li [b,c]

[a] Ministry of Education Key Laboratory of Analysis and Detection for Food Safety, Fujian Provincial Key Laboratory of Analysis and Detection for Food Safety, College of Chemistry, Fuzhou University, Fuzhou, Fujian 350002, China
[b] Food Safety Key laboratory of Zhejiang Province, College of Food Science and Biotechnology, Zhejiang Gongshang University, Hangzhou 310035, China
[c] Food Safety Key Laboratory of Liaoning Province, Bohai University, Jinzhou 121013, China
[d] Environmental Monitoring Center of Fujian Province, Fuzhou, Fujian 350003, China

ARTICLE INFO

Article history:
Received 8 January 2015
Received in revised form
2 April 2015
Accepted 13 April 2015
Available online 14 April 2015

Keywords:
Thioflavin T
G-quadruplex
Fluorescent biosensor
Terbium (III)

ABSTRACT

In this paper, a novel label-free fluorescent biosensor for terbium (III) (Tb^{3+}) was proposed based on structural conversion of G-quadruplex DNA mediated by Thioflavin T (ThT) and Tb^{3+}. In the presence of K^+, ThT could bind to K^+-stabilized parallel G-quadruplex, giving rise to high fluorescence intensity. Upon the addition of Tb^{3+}, Tb^{3+} could competitively bind to parallel G-quadruplex leading to the structural change, which resulted in fluorescence decrease. The change of fluorescence intensity ($\Delta F = F_0 - F$) showed a good linear response toward the concentration of Tb^{3+} over the range from 1.0 pM to 10.0 μM with a limit of detection of 0.55 pM. This proposed biosensor was simple and cost-effective in design and in operation with ultrahigh sensitivity and selectivity. Thus, the proposed biosensor could be a promising candidate for monitoring ultratrace Tb^{3+} in environment.

1. Introduction

Recent years, the detection of the rare earth elements (REEs), such as Terbium, has attracted a significant interest because of its important roles in geochemistry (Kay and Gast, 1973; Taylor and McLennan, 1988), bioinorganic chemistry and industrial application (Hosseini et al., 2010). Above all, terbium could be accumulated in human body from the food chain, causing serious and permanent damage to the bone marrow cells (Chen and Zhu, 2008), DNA (Zhu et al., 1997) and liver (Chen and Zhu, 2009), even at low concentrations. Thus, the detection of terbium is critical for the environment and human health. However, the chemical similarity of lanthanides makes their determination unusually difficult and complicated (Bekiari et al., 2003; Xia et al., 2000). Therefore, searching for useful methods for terbium assay has been a subject of current analytical study.

So far, most techniques for the determination of terbium are inductively coupled plasma mass spectrometry (ICP-MS) (Vicente et al., 1998), or isotope dilution mass spectrometry (ID-MS) (Goldstein and Jacobsen, 1988). However, in most cases, these methods often require sophisticated apparatus and long-time analysis, which have limited their practical applications. In recent years, some other detection methods have also been reported for the detection of terbium, such as electrochemical sensor method (Zhang et al., 2009). The method is economical, simple and easy to operate. Nevertheless, it is well known that the stability of electrochemical method is not good and needs to be improved. Thus, the development of a convenient and rapid method for the determination of terbium is of urgent need (Singh et al., 2009). In all kinds of detection techniques, fluorescent sensors, especially, label-free fluorescent strategies are one of the best choices, because they are qualified with high sensitivity, fast response, and easy online detection (Li et al., 2001). For instance, many organic small-molecule fluorescent probes have been developed for the Tb^{3+} detection (Hosseini et al., 2010; Yang et al., 2004; Amr and Essawy, 2014). These label-free fluorescent methods have good sensitivity and selectivity for Tb^{3+}, but most of them require expensive modification or complicated and time-consuming procedures for synthesis of fluorescent probes. To the best of our knowledge, this type of fluorescence strategy for assaying Tb^{3+} is under-reported and remains a great challenge.

* Correspondence to: College of Chemistry, Fuzhou University, Fuzhou, Fujian 350116, China. Fax: +86 591 87800172.
E-mail addresses: zlan@fzu.edu.cn (L. Zhang), lijr6491@yahoo.com.cn (J. Li).

http://dx.doi.org/10.1016/j.bios.2015.04.039
0956-5663/

G-quadruplexes are four-stranded nucleic acid structures formed by stacking of Hoogsteen base paired G-quartets, which are common in various guanine-rich sequences (Sinden, 1994; Davis, 2004; Neidle and Parkinson, 2002; Burger et al., 2005; Burge et al., 2006). Interestingly, with many small molecules or some metals include Tb^{3+} as a co-factor, the G-quadruplexes exhibit superior optical activity, and the formed quadruplex-binding compound could greatly enhance the fluorescence of small molecules. Given such unique property, some studies have been carried out to verify the possibility of integrating G-quadruplexes with the label free fluorescence technique for exquisite sensing of metals (Guo et al., 2012; Siters et al., 2014; Li et al., 2010a, 2010b). For instance, Guo et al. (2012) utilized N-methyl mesoporphyrin IX (NMM) to serve as a fluorescence reporter and a widely used G-quadruplex as the recognition element to develop a fluorescent biosensor for Pb^{2+} determination. However, NMM may also interact with other DNA forms like the single-stranded or duplex DNAs, which make the method nonspecific, especially in complex samples. In addition, the formation of polymorphic conformation of G-quadruplex induced by K^+ ions (Lim et al., 2009) in such biosensor may cause unstable luminescence.

Surprisingly, Mohanty et al. (2013) firstly reported that water soluble ThT was a quadruplex specific fluorogenic dye among other DNA forms including triplexes, duplexes or single-stranded structure. The G-quadruplex induced directly by ThT could generate more stable luminescence, making ThT superior to that of erstwhile quadruplex-binder dye, which could make sure the sensitivity of the sensor. Also, the unique structural selectivity of ThT for G-quadruplexes may improve the specificity of sensing. Therefore, some stable, label-free fluorescent sensors for the detection of micromolecule or DNA based on ThT directly induced conformation-specific G-quadruplex have been reported (Zhao et al., 2014). However, this type of fluorescence strategy for assaying Tb^{3+} has never been reported.

Stimulated by above study, herein a label-free fluorescent biosensor based on structural conversion of G-quadruplex DNA mediated by ThT and Tb^{3+} was developed for determination of ultratrace Tb^{3+}. Using this biosensor, it was possible to detect Tb^{3+} through a linear dynamic range of 1.0 pM to 10.0 μM with a detection limit down to 0.55 pM. In comparison with above methods, the method we proposed has obvious advantages such as simple procedures, short detection time, label-free, wide linear range and so on. In order to evaluate the applicability, the river water samples spiked with different concentrations of Tb^{3+} were detected with our biosensor and ICP-MS, respectively. The results obtained with our method were consistent with those obtained with ICP-MS. Therefore, our reported biosensor provided the possibility of monitoring ultratrace Tb^{3+} in environment. At the same time, this method may be also used to predict conformational change of G-quadruplex, which might promote the development of quadruplex-specific anticancer drugs because of their potential biological functions in vivo (Zhao et al., 2014).

2. Experimental

2.1. Reagents and apparatus

The G-rich oligonucleotide (TAG4: CTCTTTAAGGGTTAGGGTTAGGGTT AGGGTAAAAA) was synthesized by the Shanghai Sangon Biotechnology Co., which were all purified by HPLC and confirmed by mass spectrometry. The concentrations were quantified by OD260 based on their individual absorption coefficients. A stock standard solution of Tb^{3+} ions (0.01 M) was prepared by dissolving $TbCl_3 \cdot 6H_2O$ (Aladdin) in water. The 1.0×10^{-5} M stock solutions of Gd^{3+} and Dy^{3+} were prepared by dissolving Gd_2O_3 and Dy_2O_3 (Wako Pure Chemical Industries Co., Ltd., Japan) in 2% nitric acid solution. And all the working standard solutions were diluted to desired concentrations with water. ThT (3,6-dimethyl-2-(4-dimethylaminophenyl) benzo-thiazolium cation) was purchased from Sigma-Aldrich. Other chemicals were purchased from Sigma-Aldrich and used without further purification. All water used to prepare buffer solutions was obtained by using a Milli-Q water system. All measurements were performed in reaction buffer (50 mM Tris–HCl, pH 5.5) unless stated otherwise.

Fluorescence spectra were measured with a Cary Eclipse fluorescence spectrometer (Agilent Technologies). UV–vis absorbance spectra were recorded with a UV-2450 spetropho-tometer (SHIMADZU, Japan) using a quartz cell with 1.0 cm optical pathway. A Bio-Logic MOS-450 spectropolarimeter (France) was utilized to collect the circular dichroism (CD) spectra of G-quadruplex stabilized by different coordination cations. Inductively coupled plasmamass spectra were measured with Agilent 750ce mass spectrometer (USA).

2.2. Fluorescence measurement for Tb^{3+}

The 400 μL Tris–HCl working buffer (50 mM, pH 5.5) containing 1.0 μM TAG4 DNA, 0.3 μM ThT and 50 mM KCl was mixed by vortex. Then the mixtures were incubated at room temperature in dark. After a short time, different concentrations of Tb^{3+} solution were added into the mixtures and mixed by vortex. Similarly, the resulting solutions were kept at room temperature for a few minutes and transferred to a spectro fluorometer cuvette. The fluorescence spectra of the above resulted solutions were recorded in the wavelength range from 435 nm to 600 nm with the excitation of 425 nm at room temperature.

2.3. CD measurements

The CD spectra of DNA were collected with a Bio-Logic spectropolarimeter in 50 mM Tris–HCl buffer (pH 5.5). The optical chamber was deoxygenated with dry purified nitrogen (99.99%) prior to use and kept under a nitrogen atmosphere during the experiments. The spectra were measured in the wavelength range 220 − 360 nm using a quartz cuvette with 1.0 cm path length, and the response time used was 1 s. Each spectrum was an average of three measurements at 25 °C. The background of the buffer solution was subtracted from the CD data.

3. Results and discussion

3.1. Principle of sensing Tb^{3+}

The experimental principle of the fluorescent biosensor was illustrated in Fig. 1. As shown in Fig. 1, the Tb^{3+} detection system contains ThT and TAG4 DNA. As mentioned above, ThT is characterized by an obvious structural selectivity for G-quadruplexes but not for other DNA forms. Then in the presence of ThT and K^+, DNA folds into parallel G-quadruplex along with a dramatic enhancement of fluorescence intensity owing to the strong interaction among the quadruplex. However, in addition of Tb^{3+}, Tb^{3+} could competitively bind to ThT/K^+-stabilized G-quadruplex, which lead to the conformational change, showing that Tb^{3+} could transform the pre-folded parallel G-quadruplex into the antiparallel G-quadruplex, and then release ThT from the folded structure. Meanwhile, it leads to the obvious decrease in the fluorescence intensity of ThT. Using this sensing platform, an ultrahighly sensitive and selective, simple, rapid sensor for Tb^{3+} detection has been developed.

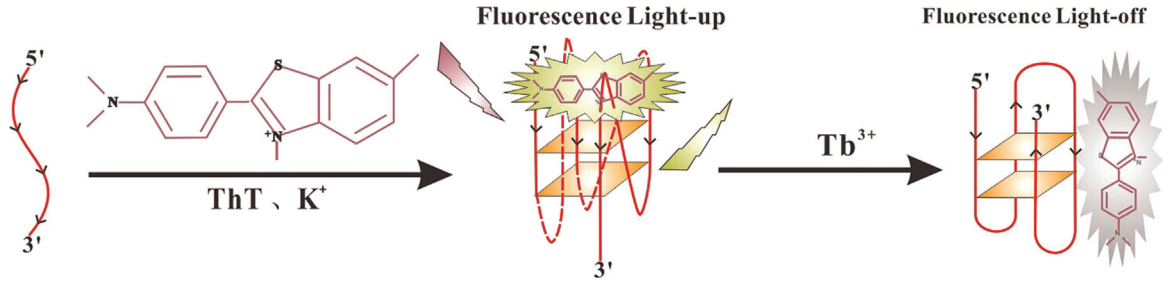

Fig. 1. Experimental principle of label-free fluorescent biosensor for ultratrace terbium.

3.2. Identification of quadruplex formation by CD

CD spectra are a very useful tool to characterize G-quadruplex. Signature CD spectroscopy have been reported for many DNA structures including double-stranded DNA and quadruplex forms (Kuang et al., 2010). So as to confirm whether the conformation of G-quadruplex was changed in the presence of Tb^{3+}, we measured the CD spectrum of DNA in the presence and absence of Tb^{3+}, respectively. As shown in Fig. 2, DNA had a characteristic CD peak at 260 nm and a trough at around 242 nm (see curve a), suggesting the base stacking and helicity structure of DNA (Balagurumoorthy and Brahmachari, 1994). Upon the addition of ThT and K^+ (curve b), a distinctive shoulder located near 270 nm on the strong positive band at 285 nm, which was the characteristic of CD spectrum of parallel G-quadruplex (Rezler et al., 2005). It maybe also suggest that the structure formed in K^+/ThT is a G-quadruplex that contains mixed parallel/antiparallel components (Rezler et al., 2005). Upon Tb^{3+} addition (curves c, d, e), the intensity of positive peak at 285 nm and negative peak at 250 nm were decreased. Tb^{3+} could competitively bind to ThT/K^+-stabilized G-quadruplex, which led to the conformational change. Furthermore, when the concentration of Tb^{3+} increased to a certain extent (curve f), a positive peak at around 295 nm, which was the characteristic of CD spectrum of antiparallel G-quadruplex (Balagurumoorthy and Brahmachari, 1994), appeared, and the band at 250 nm obviously decreased in the meantime. All above facts could indicate that Tb^{3+} induced TAG4 DNA underwent a parallel G-quadruplex to antiparallel G-quadruplex conformation transition. All above CD results confirm that our biosensor indeed work as we expect.

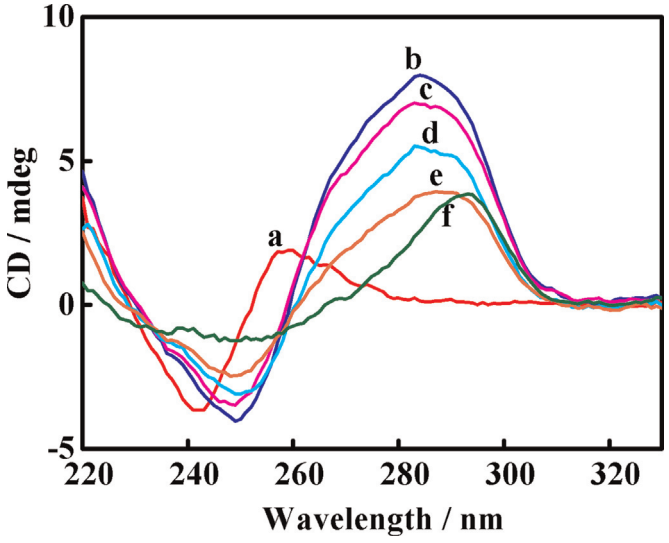

Fig. 2. CD spectra of 50 mM Tris–HCl (pH 5.5) containing 10.0 μM DNA (a), 10.0 μM DNA+3.0 μM ThT+50 mM K^+ (b), 10.0 μM DNA+3.0 μM ThT+50 mM K^+ +different concentrations of Tb^{3+}: (c) 1.0 pM, (d) 1.0 μM, (e) 0.1 mM, and (f) 1.0 mM respectively.

3.3. Identification of quadruplex formation by UV–vis and fluorescent spectrum

To further validate our method, we used the UV–vis spectrum to investigate absorbance changes of our detection system. As Fig. 3A shows, the ThT dye displayed its characteristic absorption profile with a maximum at 410 nm (curve a). The addition of DNA and K^+ led to the obvious hypochromism and bathochromic shift (the absorption peak at 410 nm shifted to 445 nm) under the same conditions (curve b). The results showed that the interaction among DNA, ThT and K^+ was strong, indicating corresponding changes of DNA conformation and structure. As discussed above, in the presence of ThT and K^+, TAG4 DNA folds into a parallel G-quadruplex structure. Because the binding sites of ThT in the quadruplexes are more specific, an obvious red shift in the UV–vis

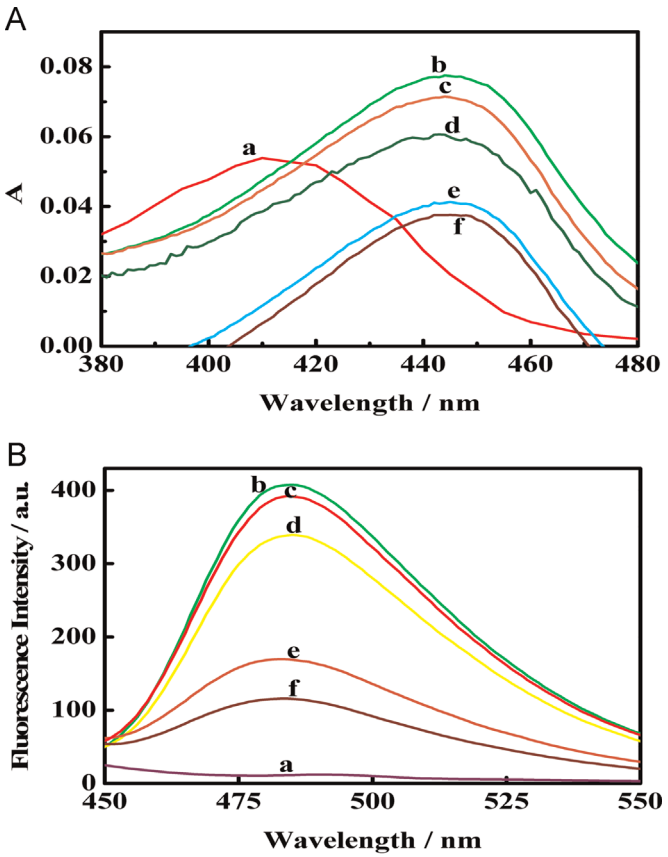

Fig. 3. (A) UV–vis spectra of 50 mM Tris–HCl (pH 5.5) containing 3.0 μM ThT (a), 3.0 μM ThT+10.0 μM DNA+50 mM K^+ (b), 3.0 μM ThT+10.0 μM DNA+ 50 mM K^++ different concentrations of Tb^{3+}: (c) 1.0 pM, (d) 1.0 μM, (e) 0.1 mM, and (f) 1.0 mM respectively. (B) Fluorescence spectra of 50 mM Tris–HCl (pH 5.5) containing 0.3 μM ThT (a), 0.3 μM ThT+1.0 μM DNA+50 mM K^+ (b), 0.3 μM ThT+1.0 μM DNA+50 mM K^++ different concentrations of Tb^{3+}: (c) 1.0 pM, (d) 1.0 μM, (e) 0.1 mM, and (f) 1.0 mM respectively.

spectrum was observed here (Neidle and Parkinson, 2002). However, the addition of Tb^{3+} led to hypochromism. And with the increase of Tb^{3+} concentration, hypochromic effect was more and more serious (curves c, d, e, and f). Tb^{3+} could competitively bind to ThT/K^+-stabilized quadruplex, which led to the conformational change. All above UV–vis results also confirm that our biosensor indeed works as we expect.

The fluorescence spectrum is also performed to serve as a proof of concept to test the approach of our design. As Fig. 3B shows, the ThT displayed a very weak fluorescent intensity (curve a). Then in the presence of DNA and K^+, DNA folded into a parallel G-quadruplex along with a dramatic enhancement of fluorescence intensity (curve b). In addition of Tb^{3+}, Tb^{3+} could competitively bind to THT/K^+-stabilized G-quadruplex, which led to the conformational change, showing that Tb^{3+} induced DNA underwent a parallel G-quadruplex to antiparallel G-quadruplex conformation transition, leading to the decrease in the emission intensity of ThT (curves c, d, e, and f). All above fluorescence measurements confirm the feasibility of our approach.

3.4. Optimization of experimental conditions

Experimental variables affecting the whole sensing process were optimized. The temperature of the detection system will directly affect conformational change of G-quadruplex. So, first, the temperature of the detection system was investigated. Figure S1A shows the relationship between the temperature of the system and the change of fluorescence response ($\Delta F=F_0-F$). From Figure S1A, it is clearly observed that the change of fluorescence intensity firstly increased and reached a maximum at 25 °C, and then decreased with the increase of the temperature. So the experiments were conducted at room temperature.

Second, pH of the buffer was also examined in detail. Figure S1B shows the relationship between the pH of buffer and the change of fluorescence response ($\Delta F=F_0-F$). From Figure S1B, the change of fluorescence response (ΔF) increased from pH 4.0 and reached a maximum at pH 5.5, followed by a decrease to pH 8.0. Accordingly, a buffer solution of pH 5.5 was selected.

Third, the change of fluorescence intensity was studied as a function of incubation time to investigate the formation of ThT-G-quadruplex complexes in the presence of Tb^{3+}. From Fig. S1C, the change of fluorescence intensity was increased until the incubation time reached 10 min in the presence of Tb^{3+}. Thus, an incubation time of 10 min was employed in the next experiments.

3.5. The sensitivity of the biosensor

The fluorescence signals toward different concentration of Tb^{3+} were measured under the optimal conditions. The fluorescence intensity decreased with increasing the concentration of Tb^{3+} (Fig. 4). Meanwhile, the change of fluorescence intensity was linear to the concentration of Tb^{3+} in the range from 1.0 pM to 10.0 μM (Fig. 4, inset) with a detection limit (taken to be three times the standard deviation of 10 blank measurements) of 0.55 pM. The above results demonstrated that the fluorescence biosensor developed in this study had a high sensitivity and a good reproducibility.

As a contrast, we studied another fluorescent biosensor for trace terbium based on Tb^{3+} promoted conformational change of TAG4 DNA G-quadruplex. Zhang et al. (2009) developed an electrochemical biosensor for the monitoring of ultratrace Tb^{3+} based on Tb^{3+} induced conformational change of G-rich DNA to form compact quadruplex. The TAG4 DNA itself has no fluorescence. However, in the presence of Tb^{3+}, the DNA changed conformation to form quadruplex and exhibited a dramatic fluorescence enhancement (Zhang et al., 2009). The fluorescence intensity

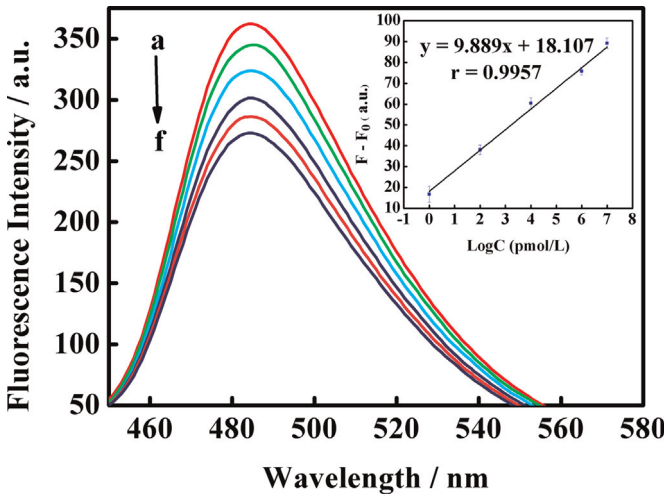

Fig. 4. Fluorescence spectra of 50 mM Tris–HCl (pH 5.5) containing 0.3 μM ThT, 1.0 μM DNA and 50 mM K^+ in the presence of 0 pM (a), 1.0 pM (b), 0.1 nM (c), 10.0 nM (d), 1.0 μM (e), and 10.0 μM (f) Tb^{3+}. F_0 and F are the fluorescence intensity in the absence and presence of Tb^{3+}, respectively. The background fluorescence of free ThT was subtracted from the sample solution.

increased with increasing the concentration of Tb^{3+} (Fig. S2). Meanwhile, the change of fluorescence intensity was linear to the concentration of Tb^{3+} in the range from 0.1 μM to 1.5 μM (Fig. S2, inset). The detection limit for Tb^{3+} was calculated to be 91 nM. This method is simple, but its selectivity remains to be improved, because other rare earth elements could also combine with DNA, which has a strong interference on the detection of terbium.

Compared with the above method, our proposed sensor has higher sensitivity and selectivity due to the high quantum yield and the photostability of ThT. At the same time, the sensor, containing no fluorescent labeling and purification process, is inexpensive and fast. Furthermore, Table S1 lists and compares with the previous Tb^{3+} sensors (Singh et al., 2009; Zhang et al., 2009; Hosseini et al., 2010; Ganjali et al., 2009; Yang et al., 2004; Zhang et al., 2011). As it is obvious, this aptasensor also exhibits higher sensitivity.

3.6. The selectivity of the method

As we all know, all lanthanides show similar chemical characteristics. In order to confirm if other members of rare earth element will interfere the detection of Tb^{3+}, Dy^{3+} and Gd^{3+} were selected as the representatives of other REEs since their chemical property is the most similar to that of Tb^{3+}. The selectivity of our biosensor was evaluated by testing the change of fluorescence response ($\Delta F=F_0-F$) in the presence of individual lanthanide's ions. As shown in Fig. 5, although the concentration of Dy^{3+} and Gd^{3+} ions was larger than that of Tb^{3+}, only Tb^{3+} caused a considerable large fluorescence response, indicating the good selectivity of our sensor. Besides, the concentration ratios of other lanthanide's ions to Tb^{3+} were much lower in nature. Therefore, Dy^{3+} and Gd^{3+} have no impact on the detection of Tb^{3+}, and other lanthanide's ions also have no effect.

We further challenged this biosensor with 0.5 nM Tb^{3+} in the coexistence of Rare Earth Multi-Element standard (REMEs). As shown in Fig. 5, the response of this biosensor to Tb^{3+} was almost unaffected by the coexistence of REMEs.

In addition, we further investigated other metallic ions such as Al^{3+}, Fe^{3+}, $Mg^{2+}$and Ca^{2+}, whose contents are higher in the Tingjiang river (Tingjiang river basin in Fujian Province is famous for its rich rare earth resources. Consequently, many rare earth industrial parks have been built along the Tingjiang river. Thus,

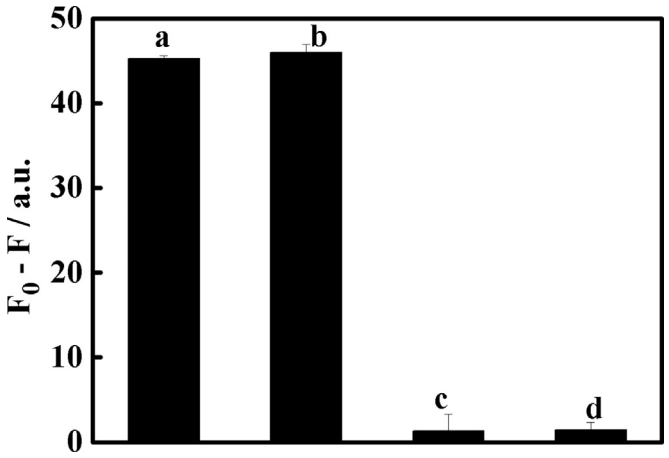

Fig. 5. Interference study. The fluorescence response ($\Delta F = F_0 - F$) in the presence of individual lanthanide's ions (a) 0.5 nM Tb^{3+}, (b) 0.5 nM REMEs, (c) 1.0 nM Dy^{3+}, and (d) 1.0 nM Gd^{3+}. F_0 and F are the fluorescence intensity in the absence and presence of Tb^{3+}, respectively.

Table 1
Determination of Tb^{3+} in artificial river water samples ($n=5$).

Tb^{3+} added (μM)	Concentration detected with this method (μM)	Recovery (%)	RSD (%)	Concentration detected by ICP-MS (μM)
0.5	0.46	92	0.58	0.52
1.0	1.10	110	0.48	0.96
2.0	2.35	117	0.32	1.93

rare earth elements could easily enter the Tingjiang river with industrial sewage discharge. Monitoring ultratrace rare earth elements in Tingjiang river is very important for the health of the people along the river.). It was found that 10,000-fold of each above metal ions (in comparison with Tb^{3+}) did not affect the current response of Tb^{3+} (signal change below 5%). It should be pointed out that 100-fold of Hg^{2+} (in comparison with Tb^{3+}) did not affect the current response of Tb^{3+} (signal change below 5%), as shown in Fig. S3. However, higher concentrations of Hg^{2+} will bring in a fluorescence quenching, which would interfere the detection of Tb^{3+}. This is mainly because TAG4 DNA contains a few T residues and it maybe form T–Hg^{2+}–T base pairs. To address the issue, we are trying to change the DNA sequence to avoid interference of Hg^{2+}, such as, replace T residues to A residues. Moreover, this interference could be overcome by introduction of a chelator that is specific for Hg^{2+}, for example, NaCN (Liu et al., 2009), KSCN (Li et al., 2010a, 2010b) and cysteine (Lin et al., 2011). More experiments are being carried out in our laboratory, in order to find a more reasonable method to avoid interference of Hg^{2+}.

3.7. Analysis of Tb^{3+} in artificial river water

Three artificial river water samples were obtained by adding different concentrations of Tb^{3+} in real river water collected in Tingjiang river (Fujian, China). The river water samples were centrifuged 30 min at 15,000 r/min and filtered by a 0.2 μm filter. Then, the concentrations of Tb^{3+} in them were determined with our method and ICP-MS. The analytical results were shown in Table 1 together with the RSD. Table 1 clearly reveals that the results obtained with our fluorescent biosensor are consistent with those obtained with ICP-MS, and have a RSD < 0.58% ($n=5$), indicating that our fluorescent biosensor has good selectivity, accuracy and reproducibility.

4. Conclusions

A label-free, simple, ultra-highly sensitive and selective fluorescent biosensor based on conformational change of G-quadruplexes for ultratrace terbium was developed here. The sensor can detect as low as 0.55 pM terbium and exhibits high discrimination ability. And the assay could be accomplished by using a common fluorophotometer. No sophisticated experimental technique or any chemical modification of DNA is required, which offers the advantages of label-free, fast, simplicity in design and in operation, and that of cost-efficiency from an application standpoint. Thus, our proposed biosensor could be a promising candidate for monitoring ultratrace Tb^{3+} in environment. At the same time, the sensor could be used to predict conformational change of G-quadruplex, which might promote the development of quadruplex-specific anticancer drugs.

Acknowledgements

The authors are grateful to National Natural Science Foundation of China (21275029), National Basic Research Program of China (No. 2010CB732403), Fujian Provincial Department of Science and Technology (2012H0005), the "12th Five-Year National Science and Technology Support Program" (2012BAD29B06), and the Program for Changjiang Scholars and Innovative Research Team in University (No. IRT1116), China.

Appendix A. Supplementary material

Supplementary data associated with this article can be found in the online version at http://dx.doi.org/10.1016/j.bios.2015.04.039

References

Amr, A., Essawy, 2014. Sens. Actuators B 196, 640–646.
Balagurumoorthy, P., Brahmachari, S.K., 1994. J. Biol. Chem. 269, 21858–21869.
Burge, S., Parkinson, G.N., Hazel, P., Todd, A.K., Neidle, S., 2006. Nucleic Acids Res. 34, 5402–5415.
Burger, A.M., Dai, F., Schultes, C.M., Reszka, A.P., Moore, M.J.B., Double, J.A., Neidle, S., 2005. Cancer Res. 65, 1489–1496.
Bekiari, V., Judeinstein, P., Lianos, P.J., 2003. J. Lumin. 104, 13.
Chen, Z.Y., Zhu, X.D., 2008. Ecol. Rural Environ. 24, 88–91.
Chen, Z.Y., Zhu, X.D., 2009. Acta Ecol. Anim. Domastici 30, 98–102.
Davis, J.T., 2004. Angew. Chem. Int. Ed. 43, 668–698.
Guo, L., Nie, D., Qiu, C., Zheng, Q., Wu, H., Ye, P., Hao, Y., Fu, F., Chen, G., 2012. Biosens. Bioelectron. 35, 123–127.
Ganjali, M.R., Veismohammadi, B., Hosseini, M., Norouzi, P., 2009. Spectrochim. Acta A 74, 575–578.
Goldstein, S., Jacobsen, S., 1988. Earth Planet. Sci. Lett. 89, 35–47.
Hosseini, M., Ganjali, M.R., Veismohammadi, B., Faridbod, F., Abkenar, S.D., Norouzi, P., 2010. Anal. Chim. Acta 664, 172–177.
Kay, R.W., Gast, P.W., 1973. J. Geol. 81, 653–682.
Kuang, H., Chen, W., Xu, D.H., Xu, L.G., Zhu, Y.Y., Liu, L.Q., Chu, H.Q., Peng, C.F., Xu, C. L., Zhu, S.F., 2010. Biosens. Bioelectron. 26, 710–716.
Lim, K.W., Amrane, S., Bouaziz, S., Xu, W., Mu, Y., Patel, D.J., Luu, K.N., Phan, A.T., 2009. J. Am. Chem. Soc. 131, 4301–4309.
Li, L., Wei, Y., Tong, A.J., 2001. Anal. Chim. Acta 427, 29–37.
Li, T., Wang, E., Dong, S., 2010a. Anal. Chem. 82, 1515–1520.
Liu, C.W., Huang, C.C., Chang, H.T., 2009. Anal. Chem. 81, 2383–2387.
Li, T., Wang, E.K., Dong, S.J., 2010b. Anal. Chem. 82, 1515–1520.
Lin, Z.Z., Li, X.H., Kraatz, H.B., 2011. Anal. Chem. 83, 6896–6901.
Mohanty, J., Barooah, N., Dhamodharan, V., Harikrishna, S., Pradeepkumar, P.I., Bhasikuttan, A.C., 2013. J. Am. Chem. Soc 135, 367–376.
Neidle, S., Parkinson, G.N., 2002. Nat. Rev. Drug Discov. 1, 383–393.
Rezler, E.M., Seenisamy, J., Bashyam, S., Kim, M.Y., White, E., Wilson, W.D., Hurley, L. H., 2005. J. Am. Chem. Soc. 127, 9439–9447.
Singh, A.K., Singh, P., Banerjee, S., Mehtab, S., 2009. Anal. Chim. Acta 633, 109–118.
Sinden, R.R., 1994. Academic Press, New York.
Siters, K.E., Fountain, M.A., Morrow, J.R., 2014. Inorg. Chem. 53, 11540–11551.
Taylor, S.R., McLennan, S.M., 1988. Handbook on the Physics and Chemistry of Rare Earth. 11. Elsevier, New York, pp. 435–479.

Vicente, O., Padro, A., Martinez, L., Olsina, R., Marchevsky, E., 1998. Spectrochim. Acta B 53, 1281–1287.
Xia, W.S.H., Schmehl, R.H., Li, C.J., 2000. Tetrahedron 56, 7045.
Yang, T., Tai, X., Qin, W., Liu, W., Tan, M., 2004. Anal. Sci. 20, 357–361.
Zhu, W.F., Xu, S.Q., Shao, P.P., 1997. Biol. Trace Elem. Res. 57, 71–77.
Zhao, D., Dong, X., Jiang, N., Zhang, D., Liu, C., 2014. Nucleic Acids Res. 42, 11612–11621.
Zhang, J., Gao, Q., Chen, P., Chen, J., Chen, G., Fu, F., 2011. Biosens. Bioelectron. 26, 4053–4057.
Zhang, J., Chen, J., Chen, R., Chen, G., Fu, F., 2009. Biosens. Bioelectron. 25, 378–382.